J Electr Eng Technol.2018; 13(6): 2254-2261
http://doi.org/10.5370/JEET.2018.13.6.2254

ISSN(Print) 1975-0102
ISSN(Online) 2093-7423

Stability Improvement of Battery Energy Storage System considering Synchronous Inductance Effect of Diesel Generator

Jongmin Jo*, Hyunsung An* and Kwan-Ho Chun†

Abstract – This paper analyzes stability of current control in respect of four cases of battery energy storage system (BESS) in a stand-alone microgrid. The stand-alone microgrid is composed of BESS, diesel generator and controllable loads, where all of them have a rated power of 50kW. The four cases are considered as following: 1) BESS with a stiff grid 2) BESS with the diesel generator 3) BESS with passive damping + diesel generator 4) BESS with active damping + diesel generator, and their stabilities are analyzed in the frequency domain and discrete time domain. The comparative analysis for four cases are verified through simulation and experiments through demonstration site of the stand-alone microgrid, where the DC link is connected to a 115kW battery bank composed of 48 lead-acid batteries (400AH/12V). Experimental results show a good agreement with the analysis.

Keywords: Battery energy storage system, Microgrid, Stability analysis, Diesel generator.

1. Introduction

Although demands for electrical energy have been consistently increased worldwide, many of the population such as developing countries are not receiving the benefits of electricity. In order for these people to use electrical energy, it is possible to expand existing electric networks or to introduce renewable energy systems based on wind turbine (WT), photovoltaic (PV) power generation. In general, it might be preferred to expand the existing electric networks, however, economic feasibility should be always considered since most of them in developing countries are resided in remote areas [1]. Furthermore, the concept of these remote areas is not limited to developing countries. In this case, a stand-alone microgrid can be recommended as an alternative, and it is considered as a small-scale distributed generation system [2, 3]. A study of microgrid has been already investigated from many researchers. The stand-alone microgrid is generally based on battery energy storage system (BESS), diesel generator (DG) and renewable energy, and BESS is the main unit among them. The primary role of BESS is to supply sinusoidal line voltage as the main source [4]. However, this can be impossible when the BESS does not generate enough output voltage because of an insufficient state of charge (SOC) of battery bank. BESS is equipped with ability to charge energy from other sources. When BESS is charged from diesel generator, a large synchronous inductance of that can cause resonance problem due to interference with LCL filter contained to BESS. Therefore, the techniques for stability improvement should be required to attenuate the resonance, and many literatures have been studied to perform that such as passive damping [5-7] and active damping [8-10]. This process needs stability analysis in order to determine damping resistor and/or damping gain as well as guarantee stable operating condition.

This paper proposes control and operation of BESS in a stand-alone microgrid. BESS operates as a main source in the stand-alone microgrid and supplies power to loads, also PV and DG operate by an auxiliary power supply of BESS in parallel. In addition, current control for ensuring the stable BESS operation in the stand-alone microgrid is analyzed. An effect of relatively large synchronous inductance on LCL filter and current control with several operating conditions are comparatively analyzed through bode plot in continuous time domain and root locus in discrete time domain. Stability and performance for current control of BESS in terms of four cases are verified through simulation and experiments based on 50kW demonstration site.

2. Configuration of Stand-Alone Microgrid

Fig. 1 shows configuration of the stand-alone microgrid which is composed of BESS, PV, diesel generator (DG) and controllable loads. BESS consists of Lead-Acid battery bank, DC-AC inverter. BESS operates as a main source in the stand-alone microgrid for supplying power to load. PV system consists of DC-AC inverter and PV array, and the load includes balanced, unbalanced and non-linear loads.

Fig. 2 shows configuration of BESS which consists of DC link, three-phase DC-AC inverter and LC (or LCL) filter, and three-phase PWM inverter is applied to transmit high quality power from battery bank and renewable energy sources.

† Corresponding Author: Dept. of Electrical and Electronic Engineering, Chungnam National University, Korea. (khchun@cnu.ac.kr)
* Dept. of Electrical and Electronic Engineering, Chungnam National University, Korea. (jmjo@cnu.ac.kr; hsan@cnu.ac.kr)
Received: April 5, 2018; Accepted: May 14, 2018

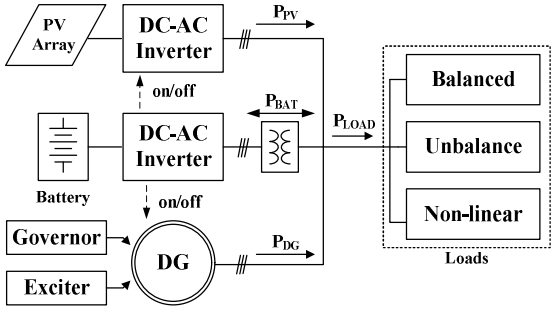

Fig. 1. Configuration of stand-alone microgrid

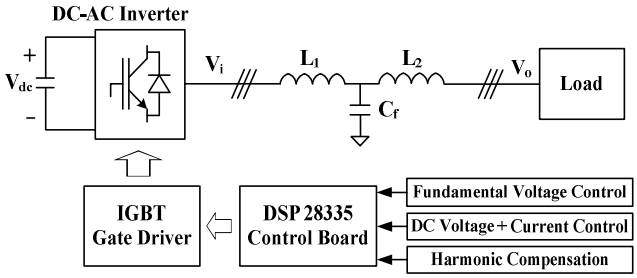

Fig. 2. Configuration of battery energy storage system

3. Control and Operation Method of BESS

Operation modes for the stand-alone microgrid are as follows. BESS supplies a microgrid voltage by PI voltage controller in the ordinary condition. On the other hand, BESS performs a current control for charging battery when SOC of battery is low condition. PV connects to BESS in parallel, and operates as grid connected mode. When power of PV is more than a load power, PV can supply a generating power to both load and BESS. DG operates in the manual mode and supplies an insufficient power in BESS. In the charge mode, DG supplies power to the load and charge to battery, simultaneously. Fig. 3 shows operation modes according to the roles of BESS, PV and diesel generator. Four modes are classified as normal, over voltage protection, charge and manual mode.

In the manual mode, diesel generator works as a main source that supplies power to loads, and BESS is charged from the diesel generator. BESS operates with the Constant Current-Constant Voltage (CC-CV) control algorithm, and performs in the grid-connected operation, where diesel generator works as a grid. As shown in Fig. 4, three-phase DC-AC inverter of BESS is a transformerless type inverter to improve system efficiency, and consists of DC link capacitor bank, six IGBTs and LCL-filter.

DC link voltage is varied by using a voltage controller as shown in Fig. 5.

The role of voltage controller is to calculate grid current command and transfer to inverter current controller shown in Fig. 6. The current controller uses PI controller with decoupling compensation in a conventional synchronous

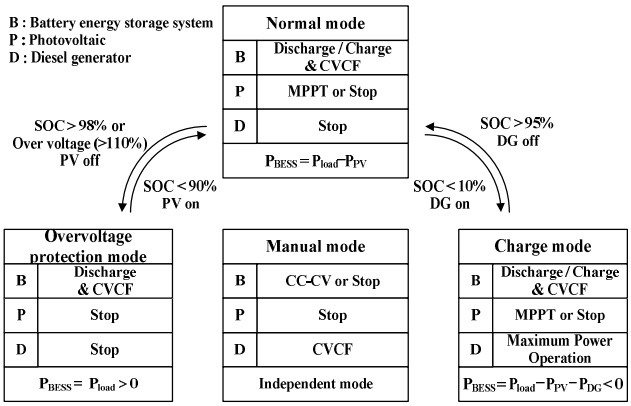

Fig. 3. Operation modes for stand-alone microgrid

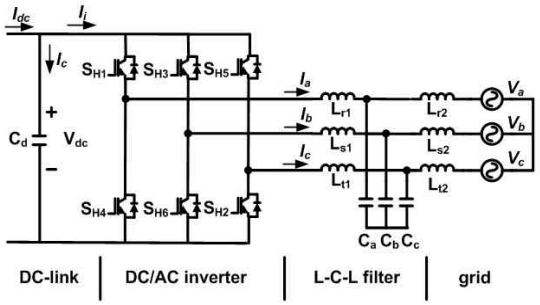

Fig. 4. Three-phase DC-AC inverter topology

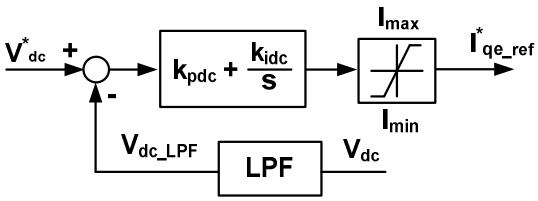

Fig. 5. DC link voltage controller

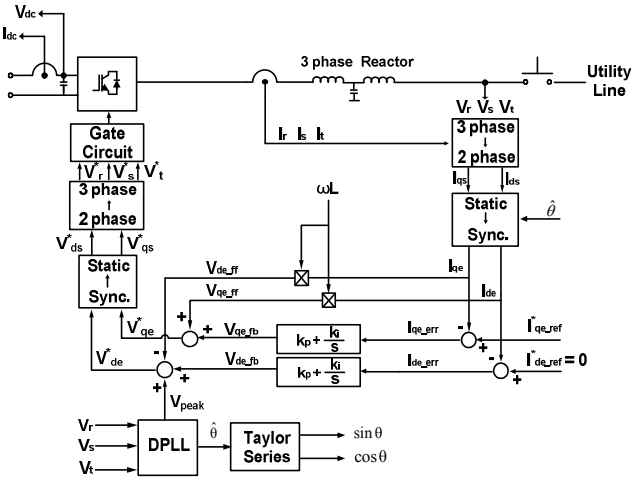

Fig. 6. DC-AC inverter current controller structure

reference frame. LCL filter with a damped resistance or current control with an active damping are employed to guarantee and improve the stable operation. Digital phase

locked loop is also designed for imbalanced grid voltage condition.

4. Stability Analysis

Table 1 shows filter parameters of BESS in which L_1 and L_2 are inverter side and diesel generator side inductances, respectively. C_f is filter capacitor and L_{DG} represents synchronous inductance of diesel generator.

Fig. 7 shows block diagram of continuous time model for current control of BESS at manual mode. The transfer function of PI + Resonant controller, system total delay and LCL filter is respectively represented by $G_c(s)$, $G_d(s)$ and $G_{LCL}(s)$.

Current control for charging SOC of battery is performed in synchronous reference frame using PI + Resonant controller. PI controller regulates fundamental positive current component and Resonant controller compensates dominant harmonics due to dead time effect for avoiding IGBT arm short, where 6th Resonant controller is adopted in this paper. Current controller is represented as follows:

$$G_c(s) = k_p\left(\frac{T_i s+1}{T_i s}\right)+\frac{k_{r6}\omega_c s}{s^2+2\omega_c s+(6\omega_0)^2}$$
$$\because\ \omega_0 = 377[rad/s] \tag{1}$$

System delay $G_d(s)$ is considered as $1.5T_s$ delay, and it consists of digital processing and PWM modulator delay as shown in

$$G_d(s) = e^{-1.5T_s s} \tag{2}$$

In this paper, grid current component is regulated as control variable, and the relationship of grid current to inverter voltage in LCL filter is derived as follows:

$$G_{LCL}(s) = \frac{I_2(s)}{V_i(s)} = \frac{1}{sL_1}\cdot\frac{z_{LC}^2}{(s^2+\omega_{res}^2)} \tag{3}$$

In this condition, z_{LC} and ω_{res} at (3) are defined as

Table 1. Filter parameter of BESS

Parameters	Symbol	Values
Inverter side inductance	L_1	1.04mH
Diesel generator side inductance	L_2	0.23mH
Filter capacitor	C_f	32uF
Synchronous inductance	L_{DG}	7.66mH

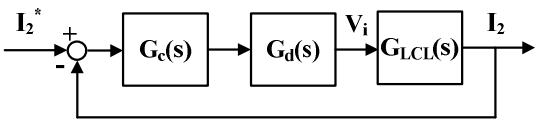

Fig. 7. Block diagram of continuous time model for current control at manual mode

$$z_{LC}^2 = \frac{1}{L_2 C_f} \quad \omega_{res}^2 = \frac{L_1+L_2}{(L_1+L_2)C_f} \tag{4}$$

To transform discrete time model from continuous time model, PI + Resonant controller is converted by tustin transformation method which has no additional phase delay when compared with continuous time modeling. System delay is substituted to one sampling time delay, transfer function of LCL filter is converted by zero order hold which contains one-half sampling time delay. From these process, open-loop transfer function in z-domain is derived in

$$G_{op}(z) = k_p\cdot z^{-1}\cdot\left\{\frac{(2T_i+T_s)z-(2T_i-T_s)}{2T_i(z-1)}\right\}\cdot$$
$$\left\{\frac{T_s}{(L_1+L_2)\cdot(z-1)}-\frac{\sin(\omega_{res}T_s)}{\omega_{res}(L_1+L_2)}\cdot\frac{z-1}{z^2-2z\cos(\omega_{res}T_s)+1}\right\} \tag{5}$$

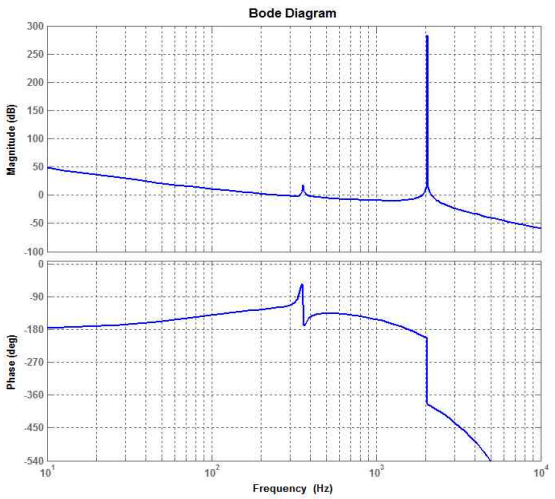

(a) Bode plot of open-loop transfer function

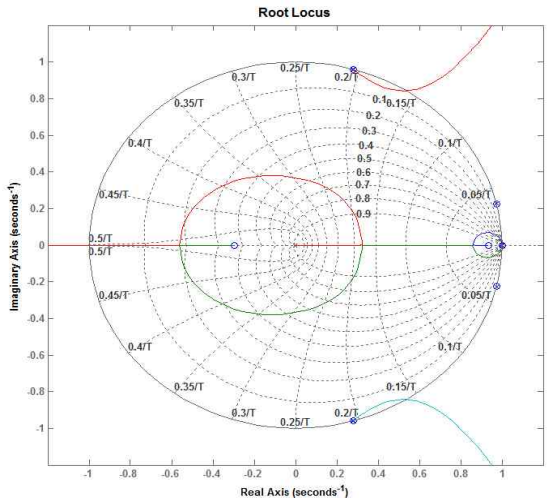

(b) Root locus of closed-loop transfer function

Fig. 8. Stability of BESS connected with stiff grid

Fig. 8(a) shows bode plot of open-loop transfer function in the s- domain, and Fig. 8(b) shows root locus in z-domain when the BESS is connected to stiff grid. Grid side inductance is L_2 and the resonance frequency is 2.05 kHz. In this condition, phase and gain margins are 62° and 8.2 dB, respectively, and thus a stable BESS operation can be guaranteed. Fig. 8(b) illustrates root locus in z-domain. The root locus shows resonance poles locate inside of unit circle when k_p is less than 5, and BESS operation is stable.

Fig. 9(a), (b) show bode plot in the s-domain and root locus in the z-domain when the BESS is connected to diesel generator, and L_{DG} represents synchronous inductance of diesel generator. In this condition, z_{LC} and ω_{res} at (3) are defined as

$$z_{LC}^2 = \frac{1}{(L_2 + L_{DG})C_f} \quad \omega_{res}^2 = \frac{L_1 + L_2 + L_{DG}}{(L_1 + L_2 + L_{DG})C_f} \tag{6}$$

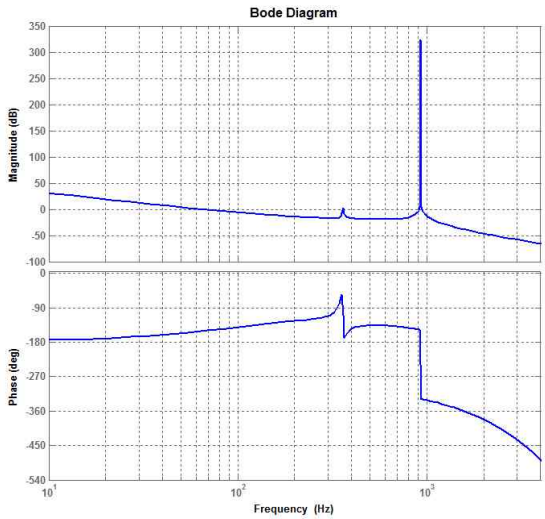

(a) Bode plot of open-loop transfer function

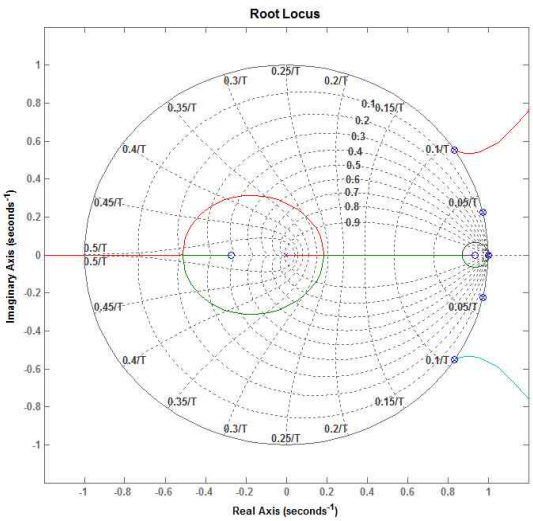

(b) Root locus of closed-loop transfer function

Fig. 9. Stability of BESS connected with diesel generator

In this case, the resonance frequency decreases to 928Hz since total grid side inductance increases to 7.89mH due to addition of the synchronous inductance. In Fig. 9(a), phase margin is reduced to 29° and gain margin is -32dB, and thus BESS operation becomes unstable due to negative gain margin. Fig. 9(b) illustrates root locus characteristic in z-domain. The root locus shows resonance poles initially locate outside of unit circle regardless of k_p gain, and BESS operation is unstable.

Fig. 10(a), (b) show bode plot in the s-domain and root locus in the z-domain when the BESS added with passive damping resistor R_d is operates with the diesel generator, where synchronous inductance of diesel generator is L_{DG}.

Since resistor R_d is added in series to the capacitor C_f in the LCL filter in order to improve current control, transfer function of LCL filter of (3) is replaced by

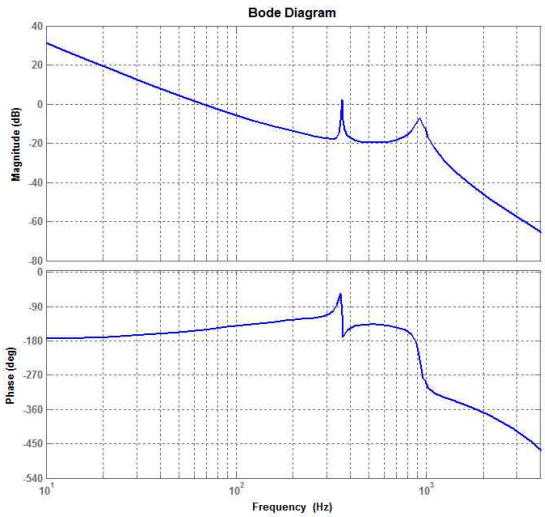

(a) Bode plot of open-loop transfer function

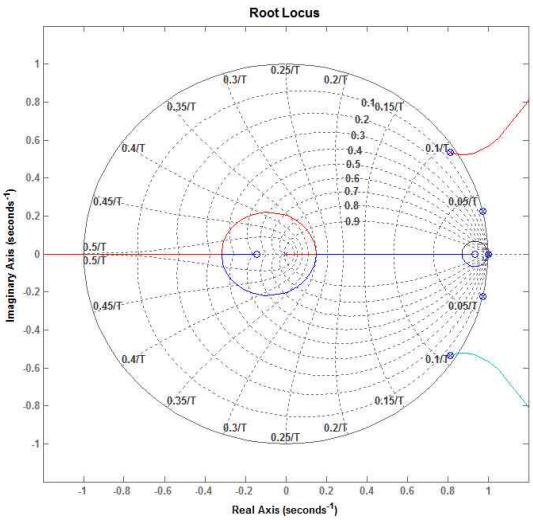

(b) Root locus of closed-loop transfer function

Fig. 10. Stability of BESS with passive damping connected with diesel generator

$$G_{LCL}(s) = \frac{1}{sL_1} \cdot \frac{\frac{R_d}{(L_2 + L_{DG})} \cdot s + z_{LC}^2}{s^2 + C_f R_d \omega_{res}^2 s + \omega_{res}^2} \quad (7)$$

Considering passive damping as shown in Fig. 10(a), phase margin is 29° and gain margin is improved to 10 dB,

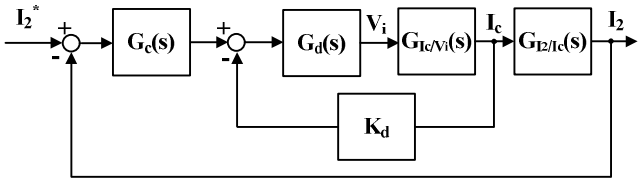

Fig. 11. Block diagram of current control considering active damping with capacitor current feedback

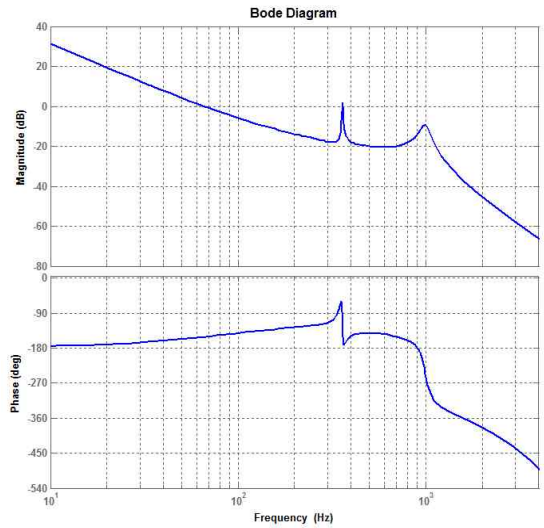

(a) Bode plot of open-loop transfer function

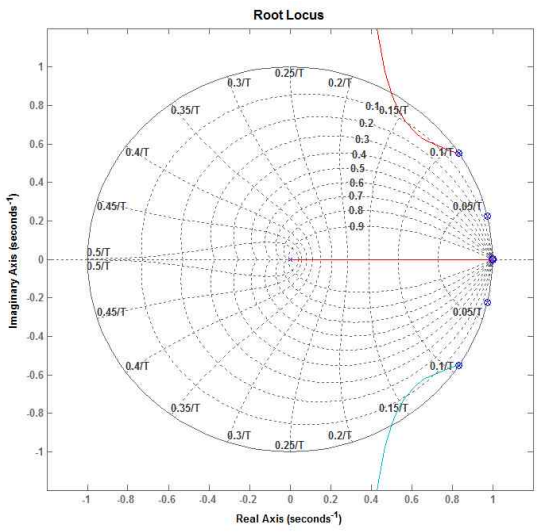

(b) Root locus of closed-loop transfer function

Fig. 12. Stability of BESS with active damping connected with diesel generator

and thus BESS operation becomes stable. Fig. 10 (b) illustrates root locus of current control in z-domain. The root locus shows resonance poles locate in unit circle when k_p gain is less than 6.4, and BESS operation is marginally stable. This contributes to the stability enhancement in current control of BESS. However, it inevitably causes the increase of power losses. To guarantee operation in the stable region, minimum value of damping resistor is derived as

$$R_{d\_\min} = k_p \frac{L_1 L_2}{(L_1 + L_2)} \quad (8)$$

An active damping method using capacitor current feedback is used to improve stability of current control as shown in Fig. 11, and transfer functions are

$$G_{Ic/Vi}(s) = \frac{I_C(s)}{V_i(s)} = \frac{1}{sL_1} \cdot \frac{s^2}{s^2 + \omega_{res}^2} \quad (9)$$

$$G_{I2/Ic}(s) = \frac{I_2(s)}{I_C(s)} = \frac{z_{LC}^2}{s^2} \quad (10)$$

Fig. 12(a), (b) show bode plot in the s-domain and root locus in the z-domain when the BESS added with active damping is connected to diesel generator. In Fig. 12(a), phase margin is 27° and gain margin is 22dB, and thus BESS operation becomes stable. The root locus shows resonance poles locate in unit circle when k_p gain locates between 0.52 and 26.1 with gain 3 at k_d. This leads to the stability enhancement of current control without any increased power losses such as passive damping method.

4. Simulation and Experimental Results

Fig. 13 shows circuit schematics for the stand-alone microgrid, where is composed of BESS with battery bank, diesel generator or stiff grid.

Fig. 14 shows simulation results of the current control of BESS, which is charging from diesel generator under different conditions. However, Fig. 14(a) shows current becomes diverged when BESS is connected with diesel generator, and highly distorted currents are supplied to BESS from diesel generator. In particular, dominant frequency component is 928Hz relevant to resonance frequency containing synchronous inductance. Fig. 14(b) shows stable current is maintained when BESS is connected with diesel generator but current control of BESS is compensated by the capacitor current feedback.

Fig. 15 shows demonstration site of the stand-alone microgrid that is composed of 50kW BESS connected to 115kW battery bank and 50kW diesel generator.

Fig. 16(a), (b) show experimental results of current control of BESS when BESS charged from diesel generator without damping and with damping, respectively. Fig. 16

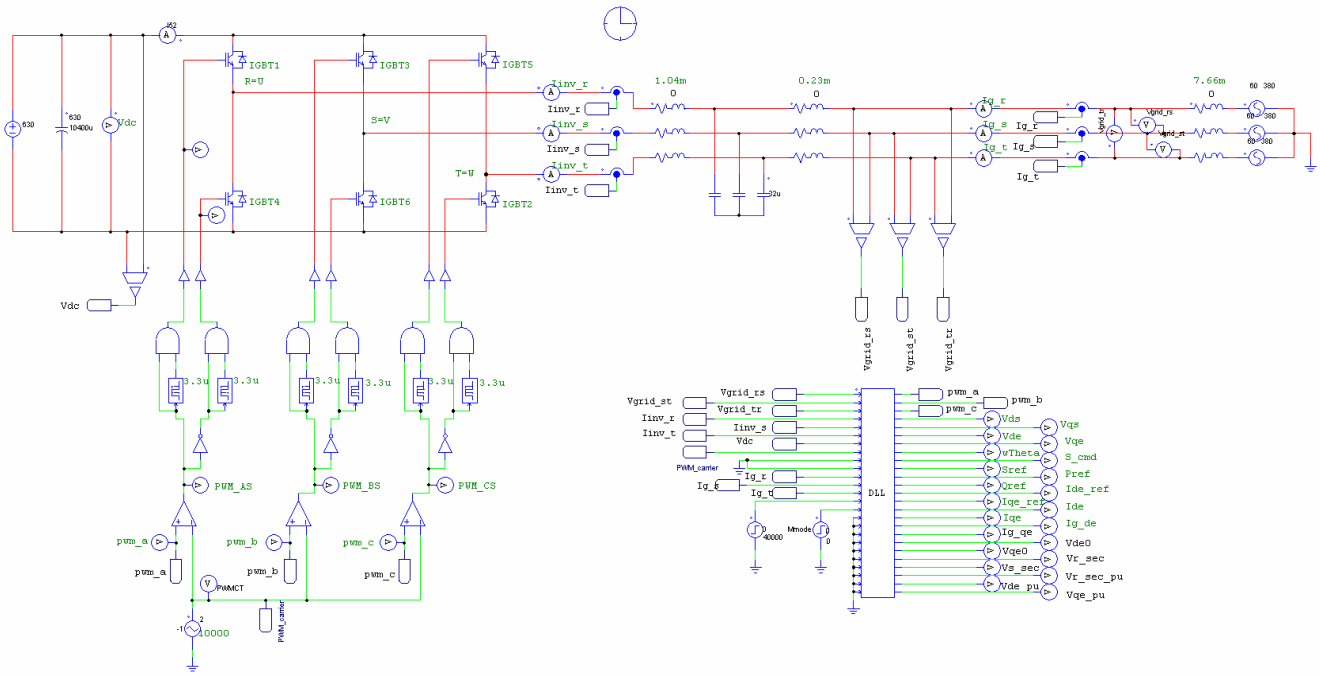

Fig. 13. Simulation of BESS and diesel generator in the stand-alone microgrid

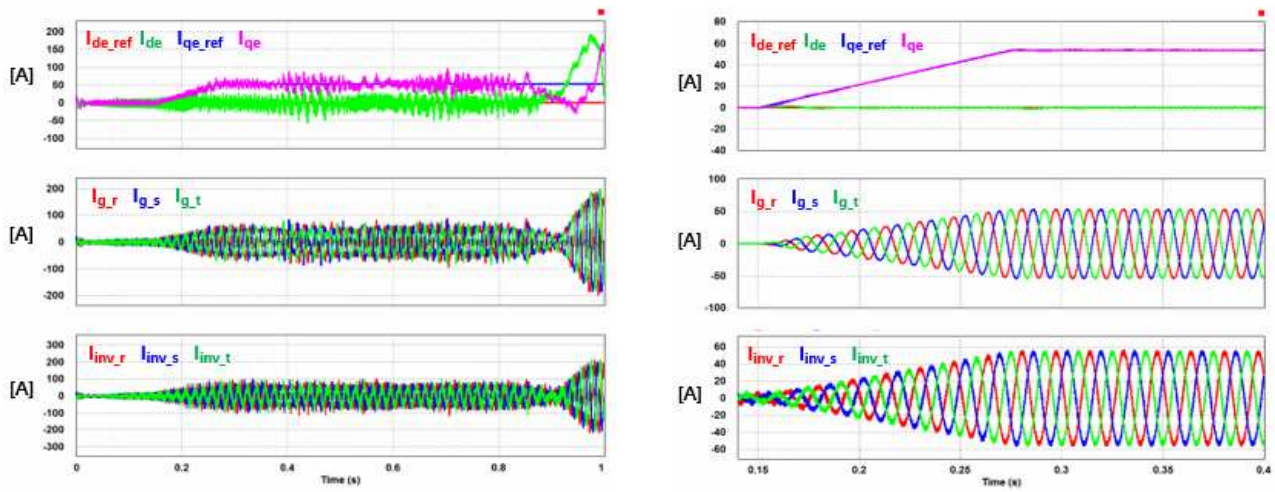

(a) Without any damping (b) With active damping

Fig. 14. Simulation results of BESS operations connected to diesel generator

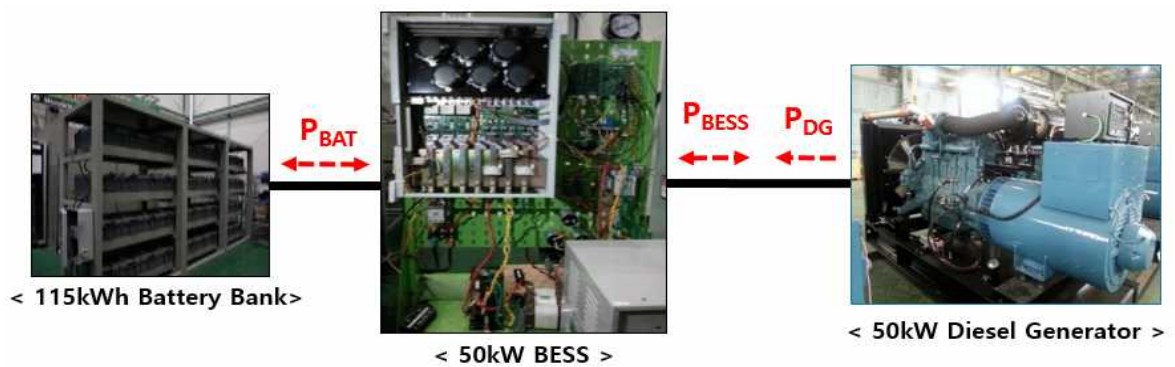

Fig. 15. Hardware configuration of BESS and diesel generator in the stand-alone microgrid

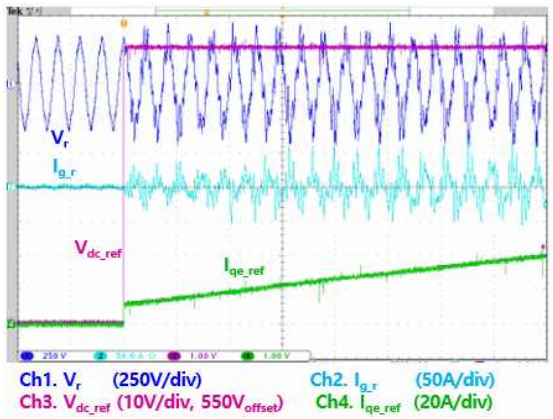

(a) Without any damping

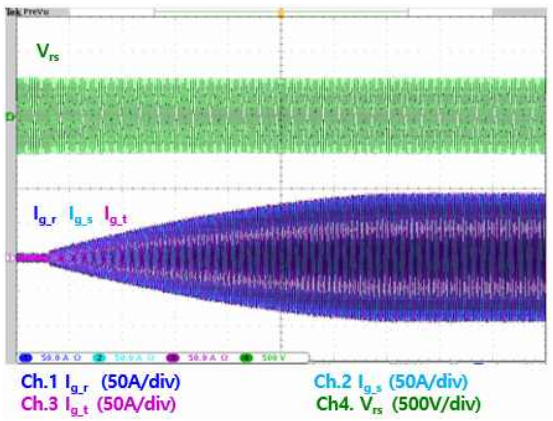

(b) With active damping

Fig. 16. Experimental results of BESS connected to diesel generator

(a) shows grid current is distorted and then BESS is tripped by over current when BESS is charged form diesel generator without any damping. In this condition, dominant frequency component causing instability of BESS is the same as the simulation result. Fig. 16 (b) shows experimental results of current control of BESS when BESS charged from diesel generator and uses the active damping method. Although resonance frequency is lowered due to the large synchronous inductance of diesel generator, charge current ramps without any effect of resonance in the transient-state and stable current flows in the steady-state. The experimental results in Fig. 16 are well matched to both the stability analysis and simulation results.

6. Conclusion

In this paper, stability of current control of BESS connected with a diesel generator for the stand-alone microgrid has been analyzed in four cases. The current control of BESS might become unstable since the large synchronous inductance caused to generate LCL filter resonance. Four cases such as stiff grid, no damping, passive and active damping method have been applied to the current control so as to compare the stability. Influence of the synchronous inductance has been investigated in the s-domain as well as the z-domain. The stable current control has been guaranteed, and current waveforms have been improved regardless of the significant synchronous inductance of diesel generator. Demonstration site for the stand-alone microgrid was established and comparative analysis for four cases have been verified through simulation and experiments, where experimental results showed a good agreement with the analysis.

Acknowledgements

This work is supported by the 2018 Open R&D Program of Korea Electric Power Corporation (KEPCO) (No. R18DO02).

References

[1] P. Bauer, L. E. Weldemariam, and E. Raijen, "Stand-alone Microgrids," *2011 IEEE 33rd Int. Telecommun. Energy Conf.* (*INTELEC*), pp. 1-10, Oct. 2011.

[2] R. J. Wai, C. Y. Lin, Y. C. Huang, and Y. R. Chang, "Design of High-Performance Stand-Alone and Grid-Connected Inverter for Distributed Generation Applications," *IEEE Trans. Ind. Electron.,* vol. 60, no. 4, pp. 1542-1555, Apr. 2013.

[3] J. Sachs and O. Sawodny, "A Two-stage Model Predictive Control Strategy for Economic Diesel-PV-Battery Island Microgrid Operation in Rural Areas," *IEEE Trans. Sustain. Energy,* vol. 7, no. 3, pp. 903-913, Jul. 2016.

[4] J. Philip, B. Singh and S. Mishra, "Design and operation for a standalone DG-SPV-BES microgrid system," *Power India International Conference* (*PIICON*), 2014 6th IEEE, pp. 1-6, 5-7 Dec. 2014.

[5] M. Liserre, F. Blaabjerg, and S. Hansen, "Design and Control of an LCL-Filter-Based Three-Phase Active Rectifier," *IEEE Trans. Ind. Appl.,* vol. 41, no. 5, pp. 1281-1291, Sep/Oct. 2005.

[6] I. Chtouki, M. Zazi, M. Feddi, and M. Rayyam, "LCL Filter with Passive Damping for PV System Connected to the Network," in *IEEE Proc. IRSEC,* Marrakech, Nov. 14-17, 2016.

[7] H. Cha and T. K. Vu, "Comparative analysis of low-pass output filter for single-phase grid-connected photovoltaic inverter," in *Proc. IEEE APEC,* Palm Springs, CA, Feb. 21-25, 2010, pp. 1659-1665.

[8] J. Dannehl, F.W. Fuchs, S. Hansen, and P.B. Thogersen, "Investigation of Active Damping Approaches for PI-Based Current Control of Grid-Connected Pulse Width Modulation Converter With LCL Filters," IEEE Trans. Ind. Appl., vol. 46, no. 4, July-Aug. 2010.

[9] X. Li, X. Wu, Y. Geng, X. Yuan, C. Xia, and X. Zhang, "Wide Damping Region for LCL-Type Grid-Connected Inverter With an Improved Capacitor-Current-Feedback Method," *IEEE Trans. Power Electron.*, vol. 30, no. 9, pp. 5247-5259, Sep. 2015

[10] D. Pan, X. Ruan, C. Bao, W. Li, and X. Wang, "Optimized Controller Design for LCL-Type Grid-Connected Inverter to Achieve High Robustness Against Grid-Impedance Variation," *IEEE Trans. Ind. Electron.,* vol. 62, no. 3, pp. 1537-1547, Mar. 2015.

Jongmin Jo was born in Korea, in 1987. He received the B.S. degree and M.S. degree in electrical engineering from Chungnam National University, Daejeon, Korea, in 2013 and 2015, respectively, where he is currently working toward the Ph.D. degree in electrical engineering. His research interests include microgrid, energy storage system, renewable energy, power quality, stability analysis, and multilevel inverter.

Hyunsung An was born in Korea, in 1985. He received the B.S. degree in physics from Chungbuk National University, Cheongju, Korea, in 2010, and the M.S. degree in electrical engineering from Chungnam National University, Daejeon, Korea, in 2013, respectively, where he is currently working toward the Ph.D. degree in electrical engineering. His research interests include microgrid, power quality, static frequency converter, motor drive system, and wave power generation system.

Kwan-Ho Chun was born in 1970, Korea. He received the B.S., M.S. and the Ph.D. degrees in Electrical Engineering from Seoul National University, in 1993, 1995 and 2002, respectively. From 2002 to 2004, he worked for SAMSUNG Electronics Co., KOREA as a senior Engineer. From 2004 to 2013, he was a senior engineer of TOSHIBA SAMSUNG Storage Technology Co., KOREA. Since 2013, he has been with the Department of Electrical Engineering at Chungnam National University, Daejeon, Korea, where he is currently an Associate Professor. His research interests include nonlinear systems theory, switched system control theory and applications in robotics, renewable energy and electrical power systems.